

Programme Area: Marine

Project: PerAWAT

# Title: A Parameterization of the end-of-Near-Wake Region for a Conventional Low Solidity and an Open-Centre High-Solidity Tidal Current Turbine

## Abstract:

This report involves the development of a parameterization for the fluid velocity field in the 'end-of-near-wake' region of a tidal current turbine wake. The parameterization links the wake velocity profile to the thrust coefficient and blockage ratio of the turbine. Separate but related parameterizations were developed for the 'conventional' low-solidity turbine of Deliverable One and the open-centre high-solidity turbine of Deliverable Two. Following this review of the literature, a new parameterization was developed based on an actuator disc blockage model, an empirical Gaussian wake velocity profile, and conservation of momentum principles. The parameterizations for the two turbines differ in the empirical velocity profile, but are otherwise based on the same fluid dynamic principles. Comparisons were made between the new parameterizations and the CFD results of Deliverables One and Two, for the two turbine geometries. A comparison was also made between the new parameterization and that used in theWind-Farmer software, for the case of the low-solidity turbine.

## Context:

The Performance Assessment of Wave and Tidal Array Systems (PerAWaT) project, launched in October 2009 with £8m of ETI investment. The project delivered validated, commercial software tools capable of significantly reducing the levels of uncertainty associated with predicting the energy yield of major wave and tidal stream energy arrays. It also produced information that will help reduce commercial risk of future large scale wave and tidal array developments.

# PerAWaT MA1003

# A parameterization of the end-of-near-wake region for a conventional low solidity and an open-centre high-solidity tidal current turbine

# WG3 WP5 D3

Dr Gareth I Gretton

The University of Edinburgh

Version: 1.0

26th February 2013

Revision history

| Version | Issue date | Summary |
|---|---|---|
| 0.1 | 28th September 2012 | First version for review by GH and consortium. |
| 1.0 | 26th February 2013 | Minor revision, for submission to ETI. |

## Executive summary

This report documents the work done for Deliverable Three of WG3 WP5 (device scale numerical modelling: detailed CFD of other concepts). Deliverable Three involves the development of a parameterization for the fluid velocity field in the 'end-of-near-wake' region of a tidal current turbine wake. The parameterization links the wake velocity profile to the thrust coefficient and blockage ratio of the turbine. Separate but related parameterizations were developed for the 'conventional' low-solidity turbine of Deliverable One and the open-centre high-solidity turbine of Deliverable Two.

As there are no existing wake parameterizations tailored to tidal current turbines, a review of the existing parameterizations for wind turbines was conducted. This included a detailed review of the parameterization used in GL Garrad Hassan's WindFarmer software. In this phase of research, it was identified that whereas wind turbine parameterizations were not sensitive to the blockage ratio of the turbine, this was likely to be a key sensitivity for tidal current turbines, and should therefore be incorporated into the model.

Following this review of the literature, a new parameterization was developed based on an actuator disc blockage model, an empirical Gaussian wake velocity profile, and conservation of momentum principles. The parameterizations for the two turbines differ in the empirical velocity profile, but are otherwise based on the same fluid dynamic principles.

Comparisons were made between the new parameterizations and the CFD results of Deliverables One and Two, for the two turbine geometries. Good general agreement was observed, with the appropriate level of sensitivity to the thrust coefficient and blockage ratio of the turbine. Further, the level of agreement between the parameterization introduced in this report and the CFD results is in line with the level of agreement seen between the wind turbine parameterizations and experimental results for wind turbines, as reported in the literature.

A comparison was also made between the new parameterization and that used in the WindFarmer software, for the case of the low-solidity turbine. This showed that the new parameterization was superior, especially for cases with higher blockage. Thus, the new parameterization represents a step forward in predictive accuracy for tidal current turbine models.

# Contents

# 1 Introduction to this document

Deliverable three of WG3 WP5 (device scale numerical modelling: detailed CFD of other concepts) is concerned with the development of a parameterization of the 'end-of-near-wake' region for tidal current turbines of 'conventional' low-solidity and open-centre high-solidity geometries. This parameterization is informed by and compared with the CFD results of deliverables one and two of this work package (Gretton, 2011a,b) which were concerned with the low-solidity and the open-centre high-solidity geometries respectively.[1]

The 'end-of-near-wake' region of a turbine is defined as being a location at which full (or practically full) pressure recovery has occurred and where the shear layers (through an initial, notionally top-hat, wake profile) have reached the centreline. These two criteria mean that the wake centreline velocity will have reached the lowest level: further upstream the lack of pressure recovery means the velocity will be higher, while further downstream mixing will have occurred and the velocity will again be higher. In practice, these criteria may not be achieved if the mixing is sufficiently strong, such that the shear layers reach the centreline before full pressure recovery is achieved.

This region is a useful upstream starting point for a wake model, because the fact that pressure recovery has been achieved means that a parabolized model can be used downstream, this being a model where pressure gradients are neglected. Further, whilst a parabolized wake model could be started at any location downstream, it is desirable to start as far upstream as possible so that inter-turbine interactions are properly modelled. End-of-near-wake parameterizations are therefore the upstream boundary conditions for a downstream wake model.

The initial acceptance criteria for this deliverable stated that the parameterization would describe the "growth, decay, width, intensity, and energy deficit of the wake". In consultation with GL Garrad Hassan, it was identified that the key variable to parameterize was the velocity deficit in the end-of-near-wake region. This velocity deficit (profile) can then be used to determine both the momentum and energy deficits of the wake, as required. Further, whilst the parameterization needs to describe the growth of the wake from immediately behind the rotor plane to the end-of-near-wake region, it is not required that the parameterization describe the growth of the wake at and downstream of this position, as this is captured by the parabolized wake model.

[1] These are henceforth referred to as the 'D1' and 'D2' reports.

In formulating a parameterization, it was considered that there were two possible approaches: one, simple ‘curve-fitting’ to the existing CFD data, and two, the use of an analytical model either as the whole or part of the parameterization. It was considered that the second approach was superior, as simple curve-fitting would struggle to capture the underlying processes, and would limit confidence in the predictive capacity of the developed parameterization. It was also considered that, given the relatively limited quantity of data available, it was preferable to have an analytical basis.

Regarding linkages and dependencies, whilst the technical contract does not list the present deliverable as being a dependency for any other work package/deliverable, it is clear that this parameterization feeds into WG3 WP4, as is stated for D4 of this work package. (WG3 WP4 is the development of the PerAWaT tool i.e. ‘TidalFarmer’.)

In the report which follows, a literature review of existing (wind turbine) wake parameterizations is first given, before proceeding to the development of the parameterizations of the two turbine geometries, which are discussed in separate sections.

# 2 Nomenclature

The nomenclature defined below is used throughout this report, including in the literature review, where it replaces the notation used by the cited authors. Notation used only briefly is introduced in the text of the report.

**Table 1:** *Nomenclature.*

| Roman symbols | |
|---|---|
| $a$ | Axial induction factor for velocity at the actuator disc |
| $b$ | Axial induction factor for velocity in the far wake in an actuator disc model, and wake half-width |
| $C$ | Tunnel or computational domain area in the blockage model |
| $D$ | Turbine diameter |
| $R$ | Turbine radius |
| $S$ | Wake area in the blockage model |
| $U(x, r)$ | Flow velocity at an arbitrary location |
| $U_0$ | Flow velocity upstream of turbine. Equivalent to $U_\infty$ for an un-blocked case. |
| $U_{ad}$ | Velocity at the actuator disc |
| $U_{bp}$ | Bypass velocity at the end of the near wake |
| $U_c$ | Wake centreline velocity at the end of the near wake |
| $U_w$ | Wake velocity at the end of the near wake |
| $U_\infty$ | Free-stream velocity |
| **Greek symbols** | |
| $\alpha$ | Blockage coefficient. $\alpha \equiv A/C$. |
| $\beta$ | Wake expansion coefficient. $\beta \equiv S/A$. Note that in the D1 report this was referred to as $\sigma$, but sigma is used for the Gaussian half-width in this report. |
| $\Delta\dot{M}$ | Momentum flux deficit |
| $\Delta\widetilde{\dot{M}}$ | Normalized momentum flux deficit. ($\Delta\widetilde{\dot{M}} = \Delta\dot{M}/(0.5\rho U_\infty^2 A_{\text{ref}})$ |
| $\Delta U$ | Velocity deficit at a given location ($\Delta U \equiv U_0 - U$) |
| $\Delta\widetilde{U}$ | Normalized velocity deficit ($\Delta\widetilde{U} \equiv \Delta U/U_0$) |
| $\sigma$ | Half-width of Gaussian profile |

# 3 Literature review

The literature on wind farm wake models, which include parameterizations of wind turbine wakes either as the whole or part of the wake model itself, are an obvious starting point for the present work. Numerous papers and reports provide an overview of the field, but a useful reference is the paper of Barthelmie et al. (2006) which covers work conducted as part of the EU-funded 'ENDOW' project (Efficient Development of Offshore Wind Farms).

This paper contains a summary of the wake models which were used and in some cases developed as part of the ENDOW project, and compares the results from the models with wind turbine data. Based on the discussion in the paper, three of the models were investigated further, and are discussed in turn below. These three models were not necessarily selected on the basis of absolute superiority, but instead on the basis of exploring concepts which were though to be most amenable to application in the present context.

A more recent paper by a similar set of authors, (Barthelmie et al., 2009), which covers work conducted as part of the EU-funded 'UpWind' project, again gives a summary of a number of wake models. In this case though, there is a shift towards CFD models of the wake, which do not feature parameterizations. It was thus concluded that the models covered in (Barthelmie et al., 2006) remain representative of the state of the art in wake parameterizations.

## 3.1 Actuator disc theory

Prior to embarking on a review of the literature, a brief re-cap is given of the most relevant definitions in, and results from, un-bounded actuator disc theory. It is given here because many of the wake parameterizations in the literature are derived, at least in part, from this theory, and it is therefore useful to have the key results as part of this document. A full description of the un-bounded actuator disc model is given in numerous references e.g. Burton et al. (2001).

The velocity at the actuator disc is defined as:

$$U_{\text{disc}} \equiv (1 - a)U_{\infty} \tag{1}$$

while the velocity in the wake, following pressure recovery, is calculated as:

$$U_{\text{wake}} = (1 - 2a)U_\infty \tag{2}$$

which can also be arranged as:

$$\Delta\widetilde{U}_w \equiv \frac{U_\infty - U_{\text{wake}}}{U_\infty} = 2a \tag{3}$$

where $\Delta\widetilde{U}_w$ is the normalized velocity deficit in the wake.

The thrust coefficient is defined as and equals:

$$C_T \equiv \frac{\text{axial force}}{\frac{1}{2}\rho {U_\infty}^2 A_{\text{disc}}} = 4a(1 - a) \tag{4}$$

which, following the substitution of Equation 3, can be rearranged to give:

$$\Delta\widetilde{U}_w = 1 - \sqrt{1 - C_T} \tag{5}$$

### 3.1.1 Correction for high thrust coefficient

The above theory is only valid for axial induction factors less than or equal to 0.5, and encompassing thrust coefficients less than one. For higher axial induction factors the theory predicts reversal of flow in the wake which is physically nonsensical. What is observed in practice is that the wake becomes strongly turbulent, and entrains fluid from outside of the wake, thereby re-energizing the fluid which has passed through the rotor-plane. This permits operation up to $a = 1$, when the rotor effectively behaves as a solid disc.

A solution for this state of turbine operation is normally found by recourse to empiricism. Analysing the experimental data of previous workers, Glauert (1926) plotted a parabolic relationship between the thrust coefficient and axial induction factor. More recent workers have used a linear relationship, as summarized by Burton et al. (2001). Such a linear relationship is plotted in Figure 1, along with the actuator disc solution given above. Unfortunately, what none of these empirical relationships give any information on is the velocity in the wake, as the momentum theory, which gives $U_{\text{wake}} = (1 - 2a)U_\infty$ no longer applies.

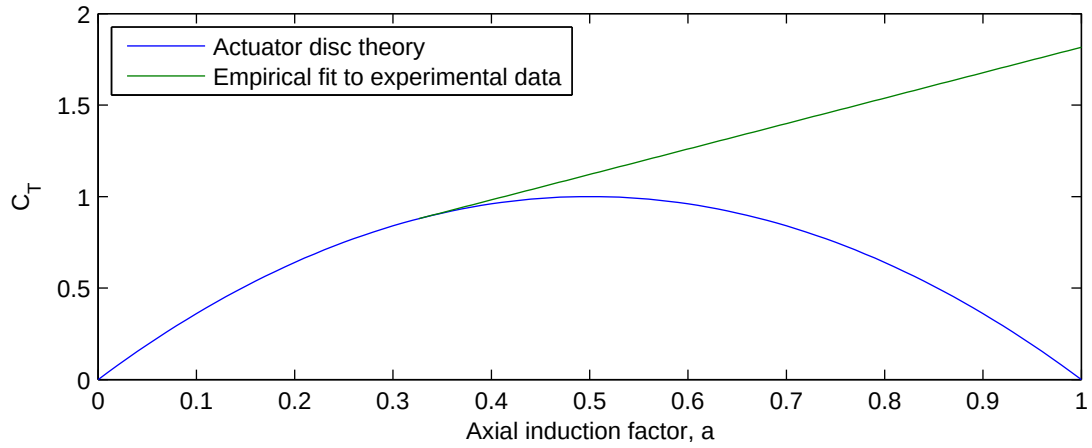


**Figure 1:** *Disc thrust coefficient versus axial induction factor from actuator disc theory and from an empirical fit to experimental data.*

### 3.2 Jensen/Katić/Risø WAsP

One of the first wind turbine wake models to be developed is that by Jensen (1983), which was later revised by Katić et al. (1986). It is used in the WAsP software from the Risø Laboratory, now part of the Technical University of Denmark (Barthelmie et al., 2006).

In this model the wake parameterization and wake model are not distinct as they are in the parameterizations/models discussed below; instead, the parameterization features a dependence on the downstream distance.

This dependence on the downstream distance is introduced by specifying that the wake diameter grows linearly:

$$D_w = D + 2kx \tag{6}$$

where $D_w$ is the diameter of the top-hat wake at an arbitrary distance downstream, $D$ is the turbine diameter, $k$ is the entrainment constant, which governs the growth of the wake, and $x$ is the distance downstream from the rotor plane.

A conservation of mass[2] analysis gives:

$$D^2 U_{ad} + ({D_w}^2 - D^2)U_\infty = {D_w}^2 U_w \tag{7}$$

[2]It is stated in the paper that this is a conservation of momentum analysis, with the assumption of straight streamlines and therefore negligible radial pressure gradients, but it is clearly conservation of mass. Given this, no assumptions need to be made about the shape of the streamlines.

Combining the above two equations, the wake deficit velocity can be found as:

$$\Delta\widetilde{U}_w = 2a/(1 + 2kx/D)^2 \tag{8}$$

were the axial induction factor is used to specify the initial velocity deficit at the rotor plane. This can be linked to the thrust coefficient using actuator disc theory i.e. $a = (1 - \sqrt{1 - C_T})/2$.

Judicious choice of the entrainment constant $k$ can lead to this model being surprisingly accurate in the context of wind farm predictions, despite the assumption of the top-hat velocity profile throughout the wake. Suggested values are 0.05 for offshore wind farms and 0.075 onshore (Barthelmie et al., 2006).

### 3.3 Ainslie

The wake parameterization of Ainslie (1988) is used in GL Garrad Hassan's WindFarmer software (Thomson, 2010) and so was of particular interest for the current work. It is also used by the University of Oldenburg's FLaP software (Lange et al., 2003). The parameterization involves an empirical relationship linking the centreline velocity deficit in the end-of-near-wake region to the thrust coefficient, and also, weakly, to the turbulence intensity of the ambient flow. A Gaussian profile is used, with the width determined from conservation of momentum considerations.

The 1988 paper does not provide any insight into the thinking behind the parameterization, but does reference a series of earlier papers Ainslie (1984, 1985, 1986) which were all examined and are discussed now in turn.

Ainslie's 1984 paper uses actuator disc theory to give the centreline velocity deficit at the end of the near wake as:

$$\Delta\widetilde{U}_c = 1 - \sqrt{1 - C_T} \tag{9}$$

i.e. the centreline value is taken to be equal to the top-hat value from actuator disc theory, Equation 5. The wake profile is given as:

$$\Delta U_w = \Delta U_c\Big(1 - (r/b)^{1.5}\Big)^2 \tag{10}$$

This profile is approximately Gaussian in shape, but gives a discontinuity in gradient at $r = 0$.

From these two equations, the wake width is then determined by conservation of momentum considerations. This, then, is a largely analytical solution, with experimental data being used to determine the profile shape.

Ainslie's 1985 paper introduces the Gaussian profile found in the 1988 paper:

$$\Delta U_w = \Delta U_c \exp(-3.56(r/b)^2) \tag{11}$$

The constant $-3.56$ in the exponential term is apparently arbitrary, and is not explained in the paper. Lange et al. (2003) however point out that the consequence of this is that at $r = b$, the velocity deficit will be 2.83% of the centreline value.[3]

With regards to the centreline velocity deficit, Ainslie states that "empirical correlations with wake data have been used to obtain initial centreline deficit as a function of the thrust coefficient" and gives the following formula:

$$C_T = 4.2\Delta U_c(2 - \Delta U_c)(0.14 - 0.125\Delta U_c)/(1 - \Delta U_c) \tag{12}$$

This of course represents $C_T$ as a function of $\Delta U_c$, and attempts by the present author to find a direct solution to the inverse function, as is required, have not met with success.

Ainslie's 1986 paper is concerned with developments to the wake model, which is a numerical model that is run using the wake parameterization as the initial conditions. No further developments to the parameterization are discussed in this, and so the 1988 paper is now considered.

As stated above, the profile given in the 1988 paper is the Gaussian introduced in the 1985 paper, Equation 11. The centreline velocity deficit is given as a function of the thrust coefficient as:

$$\Delta\widetilde{U}_c = C_T - 0.05 - (16C_T - 0.5)\frac{Ti}{1000} \tag{13}$$

Taking, for example, $Ti = 10\%$, which is somewhere towards the middle of the cases considered by Ainslie, and which range from $Ti = 2\%$ to 16%, this reduces to:

$$\Delta\widetilde{U}_c = 0.84C_T - 0.045 \tag{14}$$

[3] Were this constant defined as $-0.5$, as is used in 'standard' Gaussian profiles, the point $r = b$ would correspond to the location of the inflection point on the curve. This is close to the point at which the deficit is half of the centreline value, which occurs at $r/b = 1.177$, when the constant is $-0.5$. This is mentioned because this latter definition of the half-width is frequently used in the analysis of wakes.

Results from this have been compared with those from Equation 12 by starting with a given value of $\Delta\widetilde{U}_c$, calculating $C_T$ from Equation 12, and then re-calculating $\Delta\widetilde{U}_c$ via Equation 14. This shows that the correspondence is not 1:1, and so there is no particular link between the formulae in the two papers. This is true for all values of *Ti*.

Equation 14 may also be compared with the result from actuator disc theory, as used by Ainslie in the 1984 paper (Equation 9). This comparison is shown graphically in Figure 2, on which is also plotted a linearization of the actuator disc solution. The equation of this is

$$\Delta\widetilde{U}_c = 0.84C_T - 0.075 \tag{15}$$

which is close to the equation given by Ainslie.

The profile width is determined by conservation of momentum as:

$$b/D = \sqrt{\frac{3.56C_T}{8\Delta\widetilde{U}_c(1 - 0.5\Delta\widetilde{U}_c)}} \tag{16}$$

Finally, and with regards to the 1988 paper, it is worth highlighting that the results of Equation 13 do not appear to agree with those plotted in Figure 1 of the paper (which is mistakenly referred to in the text as Figure 2). The reasons for this are at present unclear.

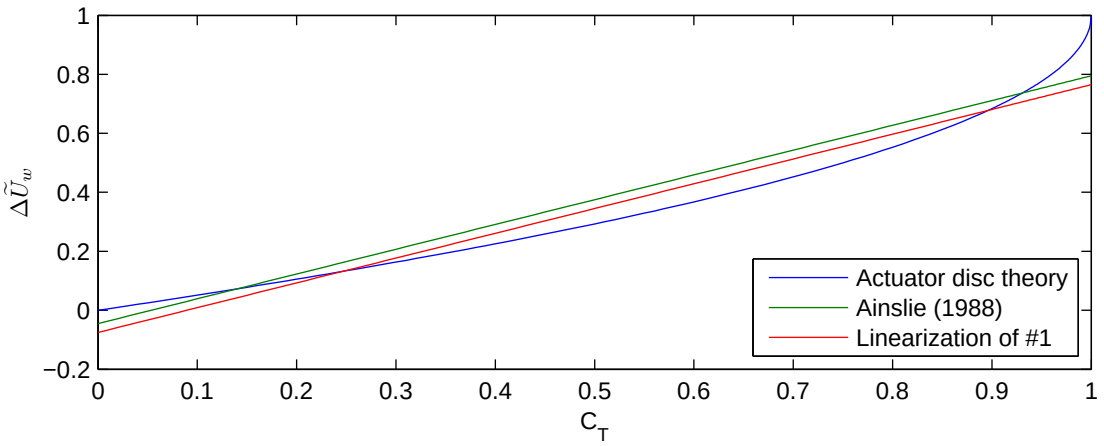


**Figure 2:** *Wake (centreline) velocity deficit versus thrust coefficient from actuator disc theory and Ainslie's parameterization. Also shown is a linear regression fit of the actuator disc solution.*

### 3.4 Schepers

As part of the EU-funded 'ENDOW' project, Schepers (2003) developed a new end-of-near-wake parameterization for the Energy Research Centre of the Netherlands' wake model. This features a Gaussian velocity deficit profile defined as follows:

$$\Delta\widetilde{U}_w = 1.3\Big(1 - \sqrt{1 - C_T}\Big)\exp\bigg(-\frac{1}{2}\Big(\frac{y}{\sigma_y R}\Big)^2\bigg)\exp\bigg(-\frac{1}{2}\Big(\frac{z - h_t}{\sigma_z R}\Big)^2\bigg) \tag{17}$$

where $y$ and $z$ are lateral and vertical coordinates and where $h_t$ is the hub-height of the turbine.

The centreline velocity deficit, $\Delta\widetilde{U}_c = 1.3(1 - \sqrt{1 - C_T})$ is derived from an actuator disc model, but tuned to fit wind tunnel measurements, while the wake half-width is calculated as $\sigma_y = \sigma_z = D_{exp}/2D$ where $D_{exp}$ is the width of the wake far downstream in the absence of mixing. This 'expanded-diameter' is calculated from the actuator disc model as:

$$D_{exp}/D = \sqrt{(1 - a)/(1 - 2a)} \tag{18}$$

What is somewhat unclear about this parameterization is how the expanded-diameter is to be calculated when the model is applied in a predictive capacity. It would appear that the only option is to calculate the axial induction factor via the thrust coefficient i.e. $a = (1 - \sqrt{1 - C_T})/2$.

With the width of the Gaussian defined as above, the normalized momentum flux deficit in the wake can be calculated as:

$$\Delta\widetilde{\dot{M}} = 8\sigma^2 1.3a(1 - 1.3a) \tag{19}$$

where the relationship between the thrust coefficient and the axial induction factor is used for brevity. This is compared with the result from actuator disc theory, Equation 4, in Figure 3. What is seen is that for low values of the axial induction factor, and hence low values of the thrust coefficient, the parameterization of Schepers under-predicts the momentum flux deficit relative to the actuator disc theory, while the reverse is true for high values of the axial induction factor.

That the normalized momentum flux deficit is no longer equal to the thrust coefficient does give the present author pause for concern. In the absence of pressure or shear forces on the external boundaries of a fluid control volume these quantities must be equal, and so the fact that they are not suggests that these pressure or shear forces must come into play, perhaps caused by the

shear of the ground boundary. This would then suggest that this process should be incorporated directly into the parameterization.

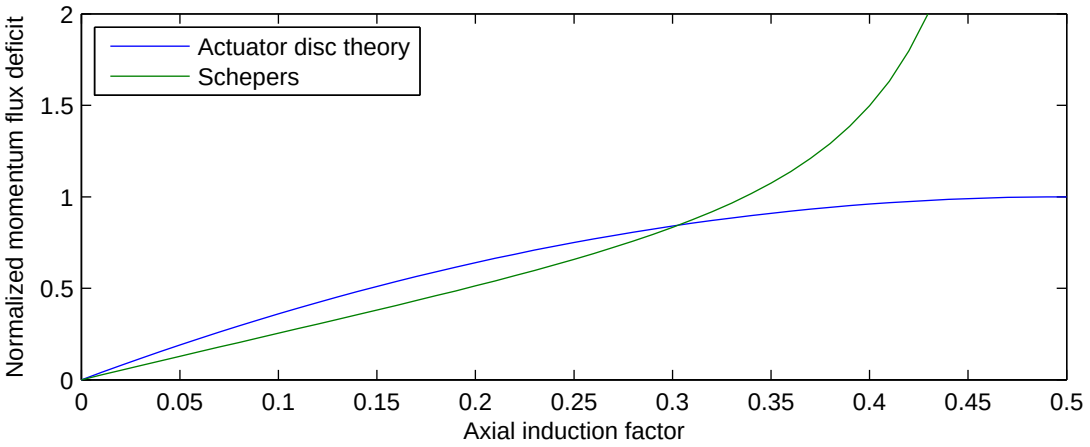


**Figure 3:** *Normalized momentum flux deficit in the wake versus axial induction factor. Results are from actuator disc theory, where the normalized momentum flux deficit is equal to the thrust coefficient, and from the parameterization of Schepers.*

## 3.5 Conclusions from the literature review

The foregoing literature review has shown that there are a number of approaches in existence for the parameterization of the end-of-near-wake region behind a wind turbine. These parameterizations generally employ a combination of empiricism and fluid dynamic modelling, with the latter encompassing actuator disc models and the law of the conservation of momentum. All parameterizations link the wake deficit to the thrust coefficient, while Ainslie's parameterization also includes a dependence on the free stream turbulence intensity.

For tidal current turbines, one of the key sensitivities is to the blockage coefficient, as shown in the D1 report. As a key illustration of this, the data from the domain radius (domain blockage) study show that, for a turbine operating at a fixed tip speed ratio relative to the upstream velocity, as the blockage ratio decreases the thrust coefficient also decreases whilst the wake deficit velocity increases. Thus, we have the opposite relationship between the thrust coefficient and the wake deficit to that given by the wind turbine parameterizations surveyed, which do not include any sensitivity to the blockage. (Note, however, that the wind turbine wake models, which are solved downstream based on the upstream boundary condition of the end-of-near-wake parameterizations, do generally consider the blocking effect of the ground.)

It was thus concluded that the effects of blockage would have to be considered for a successful tidal turbine parameterization, making this a key departure point between the models for wind and tidal current turbines. The method for this, which will be discussed in the following section, is to use the blocked actuator disc model described in Appendix B of the D1 report. This model was used in the D1 report to correct the blocked CFD simulations to free-stream conditions, but the solution of the model provides a 'top-hat' wake profile. This can be used as the basis of an empirical Gaussian profile, where the maximum value of the Gaussian is determined from the top-hat wake deficit, as per Schepers (2003), and the width of the Gaussian is determined by conservation of momentum considerations, as per Ainslie (1988).

# 4 Parameterization of low-solidity turbine results from D1

As discussed in the conclusions to the literature review, the use of a blockage model was identified as a key requirement for the parameterization of the end-of-near-wake region. Further, the blockage model described in Appendix B of the D1 report can be used for this purpose. This model is therefore reviewed before proceeding to a description of the parameterization derived from it.

## 4.1 Blockage model

The blockage model described in Appendix B of the D1 report was previously used to calculate equivalent un-blocked values of the thrust coefficient, power coefficient, and tip speed ratio from those values derived from the blocked CFD simulations. The key variable from the blockage model which allows for the calculation of this correction is the velocity at the actuator disc in the blocked case, but the velocity in the far wake (that is, after pressure recovery, but in the absence of mixing) and the velocity in the bypass flow are also solved for. These velocities are labelled $u$, $u_1$, and $u_2$ in Figure 4.

Results from this model were not presented in the D1 report as it was used purely to obtain the blockage correction factors. As such, results are presented here in Figure 5. This shows the normalized deficit velocities at the actuator disc, in the wake, and in the bypass flow, derived from $u$, $u_1$, and $u_2$. Note that the 'deficit' velocity for the bypass flow is negative as the bypass

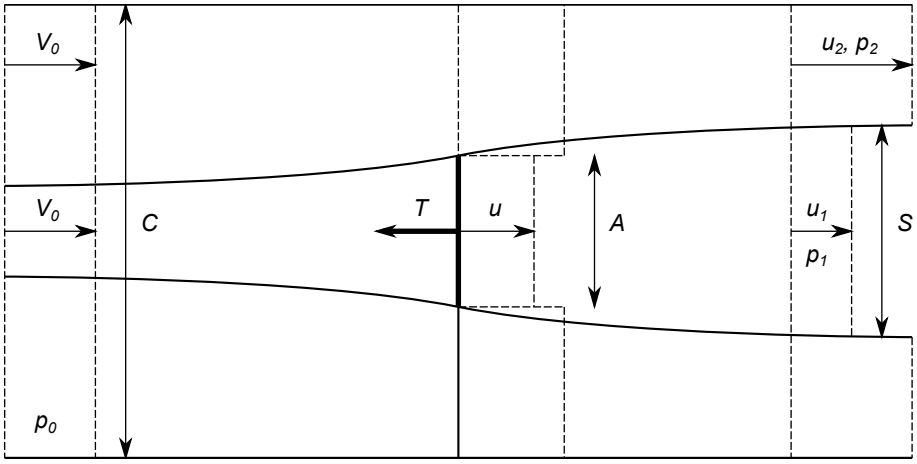


**Figure 4:** *Diagram showing streamlines and velocities for a turbine in a wind tunnel, after Mikkelsen (2003). See Appendix B of the D1 report for a full description of the nomenclature.*

flow is accelerated. Also shown are the wake expansion ratio[4] $\beta = S/A$, and the induction factor ratio $b/a = \Delta\widetilde{U}_w/\Delta\widetilde{U}_{ad}$. All variables are plotted as a function of the thrust coefficient and for un-blocked flow and three different blockage ratios. The blockage ratios correspond to those used in the CFD studies in D1.

Clearly there is a trend whereby the departure from un-blocked conditions increases progressively as the blockage is increased, and as the thrust coefficient increases. Certainly for the highest blockage ratio considered, which is characteristic of the vertical blockage of current designs, and for thrust coefficients above around 0.8, the effects of blockage are considerable.

The figures are largely self-explanatory, but it is worth highlighting the fact that the effect of blockage is to *decrease* the velocity deficits $\Delta\widetilde{U}_{ad}$ and $\Delta\widetilde{U}_w$ and to also *decrease* the wake expansion. Thus the effect of blockage is to decrease the momentum flux deficit in the wake. The velocity of the bypass flow is seen to increase with blockage as would be expected. Finally, the ratio $b/a$ shows that the effect of blockage is to decrease the velocity change from the actuator disc to the far wake, relative to the velocity change from upstream to the disc. For the unblocked actuator disc this ratio is always 2, but as the blockage and thrust coefficient increase this ratio becomes smaller.

The momentum flux deficit in the wake can be calculated from the above variables, as follows, starting with the definition of the momentum flux deficit:

$$\Delta\dot{M} = \rho S\, U_w(U_0 - U_w) \tag{20}$$

Substituting the definition of the velocity deficits and the definition of the wake expansion ratio $\beta = S/A$ gives:

$$\Delta\dot{M} = \rho\beta A {U_0}^2 \Delta\widetilde{U}_w(1 - \Delta\widetilde{U}_w) \tag{21}$$

This can then be normalized by $0.5\rho A U_0^2$ to give:

$$\Delta\widetilde{\dot{M}} = 2\beta\Delta\widetilde{U}_w(1 - \Delta\widetilde{U}_w) \tag{22}$$

As a final comment on the blockage model, it is worth pointing out that, as the model (correctly) includes a net pressure drop from upstream of the turbine to downstream, the momentum flux

[4] $\sigma$ was previously used for this variable, but as this is used to represent the width of a Gaussian, we use here $\beta$ instead.

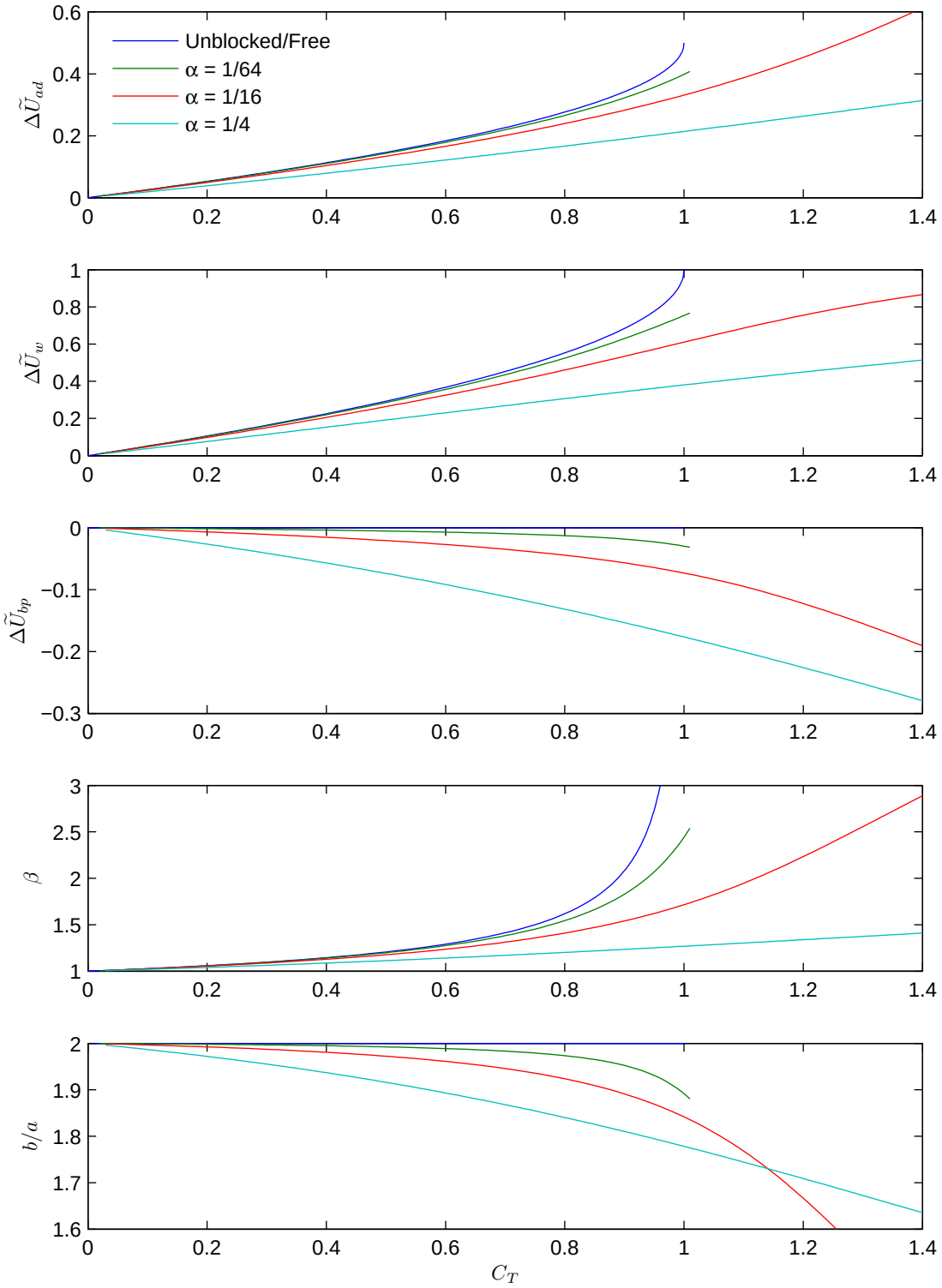


**Figure 5:** *From top to bottom: velocity deficit at the actuator disc, in the wake, and in the bypass flow, wake expansion ratio, and induction factor ratio, all versus the thrust coefficient, for unblocked flow and for three different blockage ratios, as indicated in the legend.*

deficit in the wake is no longer equal to the thrust on the turbine, as is the case for unblocked flow.

## 4.2 Wake profile

In the wake parameterization introduced below, the wake velocity deficit $\Delta\widetilde{U}_w$, bypass velocity deficit $\Delta\widetilde{U}_{bp}$, and wake expansion factor $\beta$ from the blockage model serve as the basis for an empirically-derived Gaussian profile. This follows the model of Schepers (2003), where the maximum value of the Gaussian is based on the wake deficit from an actuator disc model, and the model of Ainslie (1988), where the width of the Gaussian is determined by conservation of momentum considerations.

A Gaussian may be fitted to the top-hat wake of the blockage model in a number of ways, but the option chosen is to use a single Gaussian offset from the $\Delta U = 0$ axis by the value of the bypass velocity deficit, and with maximum value (relative to the 'base') equal to the difference between the wake deficit and the bypass deficit i.e.:

$$\begin{aligned}\Delta\widetilde{U}_w &= (\Delta\widetilde{U}_{w\sqcap} - \Delta\widetilde{U}_{bp\sqcap})\exp\left(-\frac{1}{2}\left(\frac{r}{\sigma R}\right)^2\right) + \widetilde{U}_{bp\sqcap} \\ &= A_1\exp(-Br^2) + A_2\end{aligned} \tag{23}$$

where:

$$A_1 = \Delta\widetilde{U}_{w\sqcap} - \Delta\widetilde{U}_{bp\sqcap} \tag{24}$$

$$A_2 = \Delta\widetilde{U}_{bp\sqcap} \tag{25}$$

$$B = 1/(2\sigma^2R^2) \tag{26}$$

Note that the subscript $\sqcap$ is used to indicate top-hat velocity profile values which are calculated by the blockage model.

As stated above, the width of the Gaussian is determined by equating the momentum flux deficit of the Gaussian with that from the top-hat profile (Equation 22). The momentum flux deficit of the Gaussian is determined by integration:

$$\Delta\dot{M} = \int_{r^-}^{r^+} \rho 2\pi r U_w(U_0 - U_w)\,\mathrm{d}r \tag{27}$$

The lower limit, $r^-$ is equal to zero, while the upper limit, $r^+$, is found by equating Equation 23 to zero i.e.:

$$0 = A_1 \exp(-Br^2) + A_2 \tag{28}$$

which can be re-arranged to yield:

$$r^+/R = C_1\sigma \tag{29}$$

where:

$$C_1 = \sqrt{-2\ln\left(\frac{-A_2}{A_1}\right)} \tag{30}$$

Returning to the integral, and substituting in the definitions of the velocity deficits, gives:

$$\Delta\dot{M} = \rho 2\pi {U_0}^2 \int_{r^-}^{r^+} r\Delta\widetilde{U}_w(1 - \Delta\widetilde{U}_w)\,\mathrm{d}r \tag{31}$$

Substituting then the definition of the wake profile, Equation 23, gives:

$$\Delta\dot{M} = \rho 2\pi {U_0}^2 \int_{r^-}^{r^+} r(A_1 \exp(-Br^2) + A_2)(1 - A_1 \exp(-Br^2) - A_2)\,\mathrm{d}r \tag{32}$$

Utilizing the result:

$$\int r\exp(-Br^2)\,\mathrm{d}r = -\frac{\exp(-Br^2)}{2B} \tag{33}$$

we can integrate the preceding equation to give:

$$\begin{aligned}\Delta\dot{M} = \rho 2\pi {U_0}^2 \Bigg[ & \frac{1}{2B}(2A_1A_2 - A1)\exp(-Br^2) \\ & + \frac{{A_1}^2}{4B}\exp(-2Br^2) + \frac{1}{2}(A_2 - {A_2}^2)r^2 \Bigg]_{r^-/R}^{r^+/R}\end{aligned} \tag{34}$$

Following substitution of $B = 1/(2\sigma^2R^2)$, this can be normalized to give:

$$\begin{aligned}\Delta\widetilde{\dot{M}} = \Bigg[ & 4\sigma^2(2A_1A_2 - A1)\exp\left(-\frac{1}{2}\left(\frac{r}{\sigma R}\right)^2\right) \\ & + 2{A_1}^2\sigma^2\exp\left(-\left(\frac{r}{\sigma R}\right)^2\right) + 2(A_2 - {A_2}^2)\left(\frac{r}{R}\right)^2 \Bigg]_{r^-/R}^{r^+/R}\end{aligned} \tag{35}$$

This integral, following substitution of the limits $r^-/R = 0$ and $r^+/R = C_1\sigma$, can be equated with the momentum flux deficit from the top-hat profile, Equation 22, in order to calculate the width of the Gaussian profile, $\sigma$:

$$\sigma^2 = \frac{\Delta\widetilde{\dot{M}}_{\sqcap}}{4\Big(2A_1A_2 - A_1\Big)\Big(\exp(-0.5{C_1}^2) - 1\Big) + 2{A_1}^2\Big(\exp(-{C_1}^2) - 1\Big) + 2(A_2 - {A_2}^2){C_1}^2} \tag{36}$$

This completes the specification of the profile, which is now compared with the results from D1.

## 4.3 Comparison with D1 results

The CFD studies documented in the D1 report included two parametric studies with which we can compare the wake parameterization introduced above. These are, a study of the effect of the blockage ratio, and a study of the effect of tip speed ratio. In both cases all other variables were held constant, that is, in the blockage ratio study the tip speed ratio was 5, while in the tip speed ratio study the blockage ratio was 1/16.

Considering first the study of the blockage ratio, a comparison of lateral profiles at four downstream locations is made between the CFD and the parameterization in Figure 6. This comparison is made at four downstream locations because the current parameterization, as with the majority of those for wind turbines, does not fix the downstream location at which it is to be applied. Instead, and as discussed in the introduction to this document, it is to be applied at a point where pressure recovery has occurred and where the shear layers have grown through the wake; a point which in practice can only ever be approximate.

Agreement is seen to be best at $x/D = 1.0$, and is the poorest for the most highly blocked case. The centreline velocity deficit, which in the case of the CFD data is influenced by the presence of the nacelle, is generally well represented by the parameterization, with the correct trends being predicted. For the two least blocked cases the width of the Gaussian wake appears to well represent the CFD. For the profiles further downstream, the CFD data is showing substantial mixing and therefore a reduction in the velocity deficit; as such it is as expected that the agreement becomes poorer. Interestingly though, the profiles are not rapidly progressing towards a Gaussian shape.

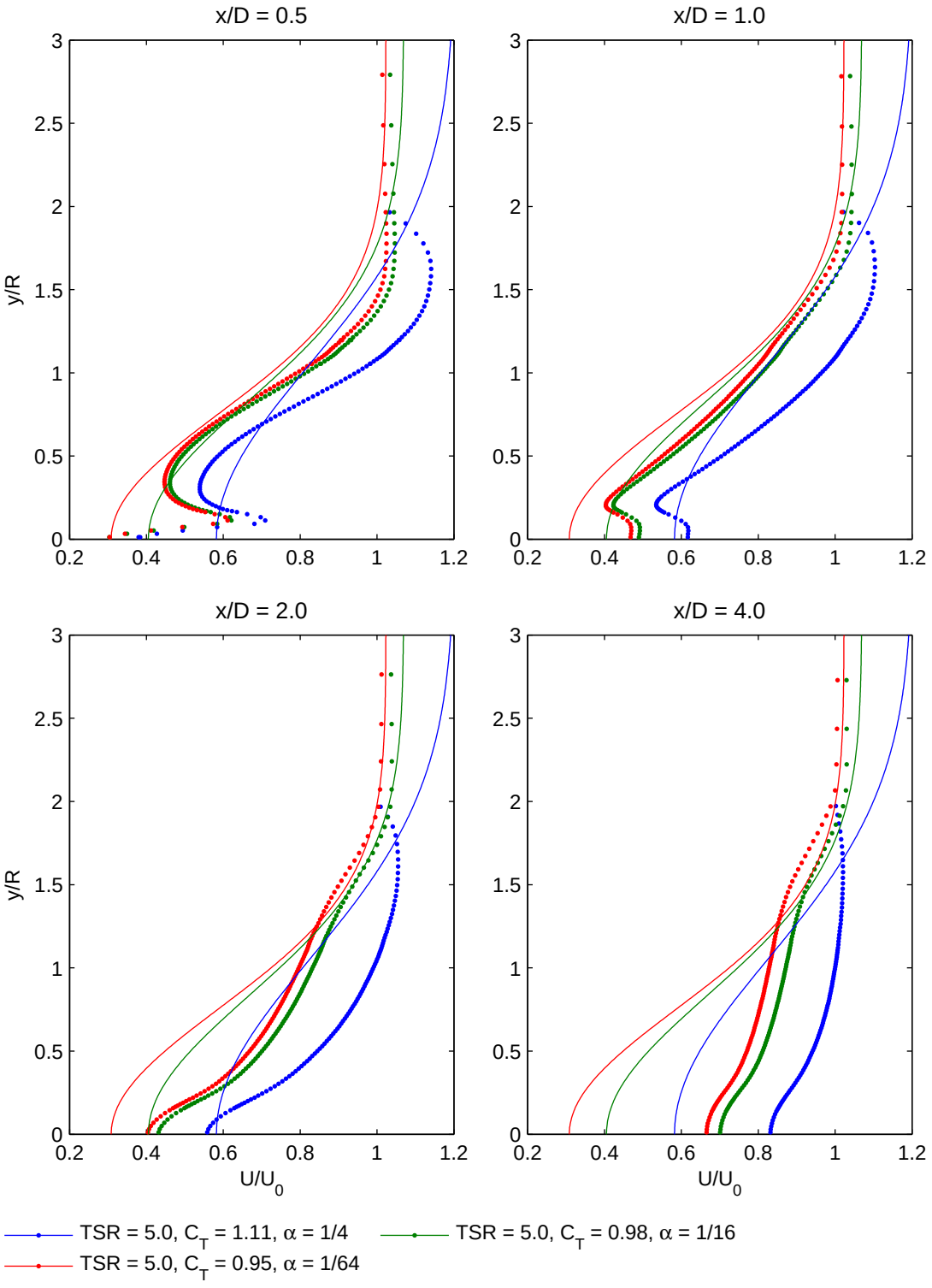


**Figure 6:** *Lateral wake profiles at four downstream locations, as indicated by the axes titles, and for* three different blockage ratios/thrust coefficients*, as indicated by the legend. CFD data are give by dots while the parameterization is given by the continuous line. Note also that the thrust coefficient varies with the blockage ratio despite the tip speed ratio being held constant.*

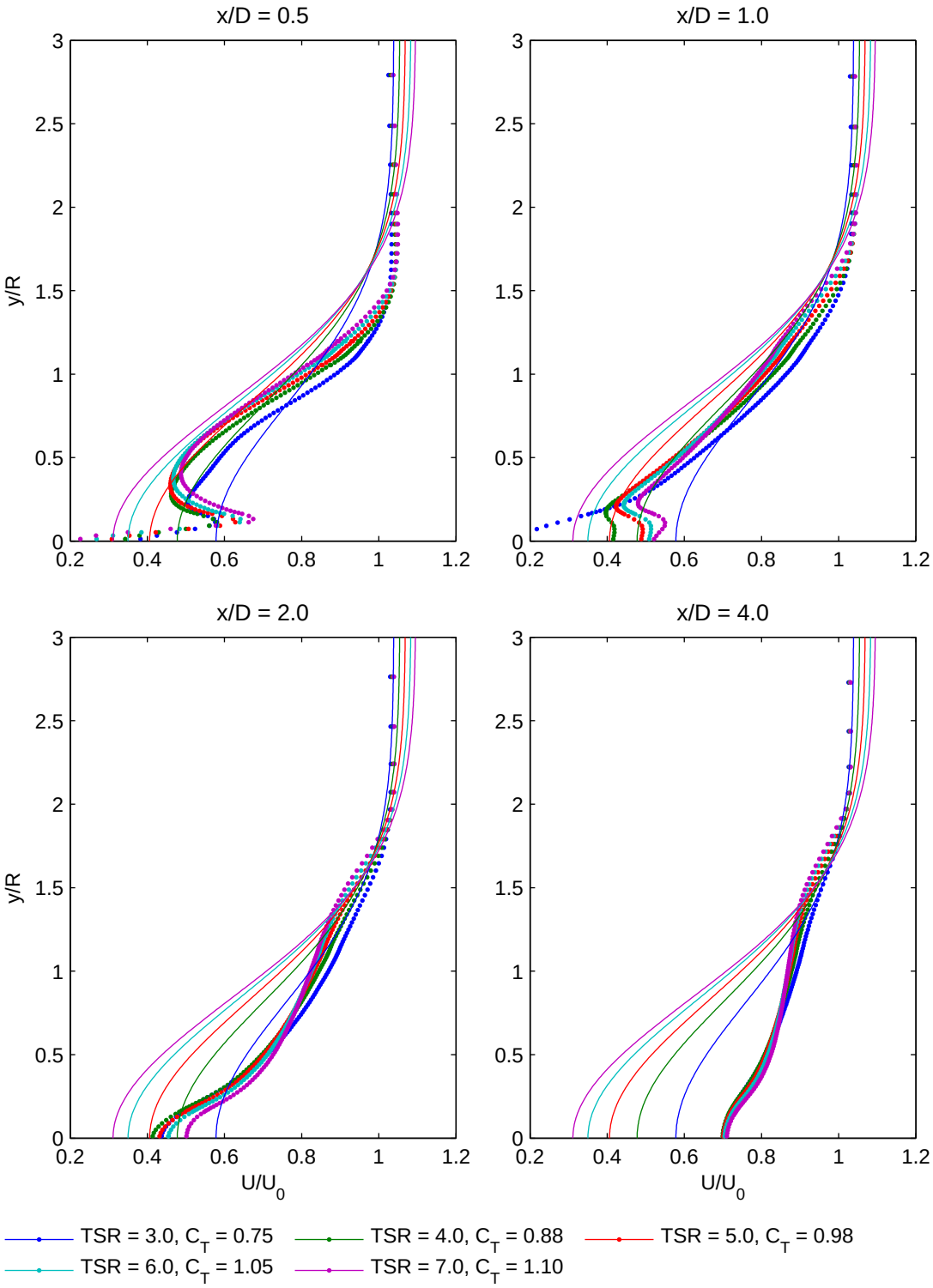


**Figure 7:** *Lateral wake profiles at four downstream locations, as indicated by the axes titles, and for* five different tip speed ratios/thrust coefficients*, as indicated by the legend. CFD data are give by dots while the parameterization is given by the continuous line.*

The poorer agreement for the most highly blocked case is likely to be due in part to a known deficiency in the means by which the Gaussian profile is fitted to the results in the blockage model. As detailed above, the width of the Gaussian is determined by conservation of momentum considerations, but no constraint is imposed for the mass flow rate or momentum flow rate of the bypass flow. This leads to the bypass flow not being correctly represented, which is most significant for this highly blocked case.

A comparison with the CFD data from the tip speed ratio study is made in Figure 7 in the same format to the above. Agreement is again best at $x/D = 1.0$, although, and as has been highlighted previously, the CFD data show an inverse relationship between the thrust coefficient and the centreline velocity deficit. Clearly the parameterization gives a direct relationship for this, which matches the CFD for $y/R > 0.75$. Agreement again becomes poorer downstream for the reasons noted above.

Overall it is considered that the present parameterization gives a good representation of the wake for the cases considered. The parameterization could potentially be 'tuned' to fit the CFD data more closely by adding adjustment factors to the centreline velocity deficit, bypass flow acceleration and width. This was done by Schepers (2003) to fit the parameterization introduced there to wind tunnel data. However, this has not been done here as the use of adjustment factors will be considered when parameterizing the effect of ambient turbulence in the work of D4.

## 4.4 Comparison with results from Ainslie's parameterization

The new parameterization introduced in the present report can also be compared with that of Ainslie (1988). Ainslie's parameterization was selected as a reference point because, as noted above, it is currently used in GL Garrad Hassan's WindFarmer software. There was thus a clear desire to understand whether, or in which cases, the new parameterization represented an improvement over Ainslie's, for the turbine cases considered in the present work.

The comparisons are made in Figure 8 for cases from the CFD blockage ratio study, and in Figure 9 for cases from the CFD tip speed ratio study. Note that each of these two figures run over two pages, and also include the CFD results. Thus, these new figures contain all of the results in Figures 6 and 7, but in a different arrangement, and with the addition of the results from Ainslie's parameterization.

Generally, the new parameterization is seen to out-perform that of Ainslie, with the differences most significant for the case with the highest blockage ratio (Figure 6, top row). This is as expected, given that the parameterization of Ainslie is intended for low blockage ratio wind turbine predictions. It might also be pointed out that as Ainslie's parameterization gives higher velocity deficits in the wake relative to the new parameterization, it is not the case that Ainslie's parameterization is better matched to the CFD results further downstream, for example.

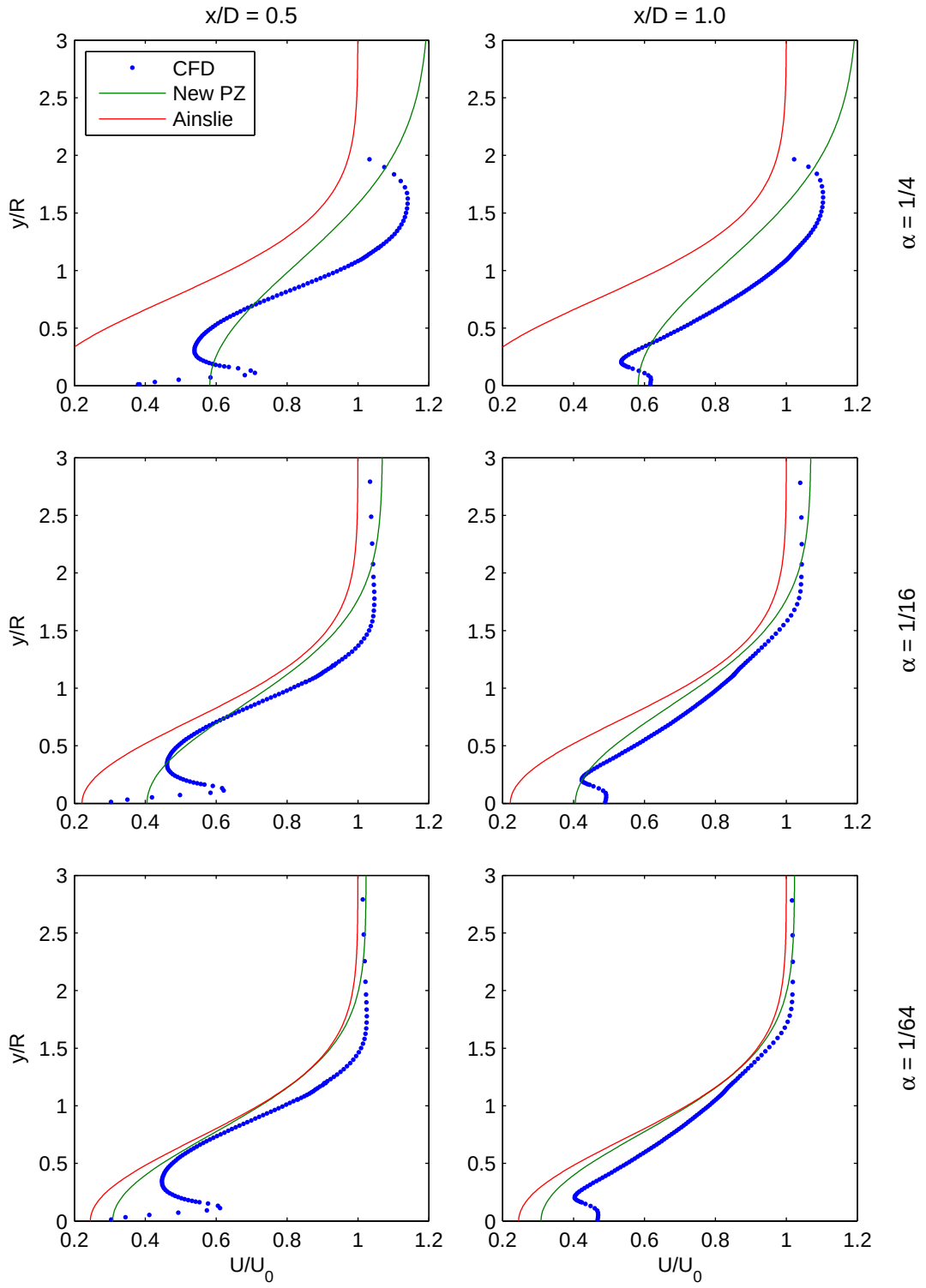


**Figure 8:** *Lateral wake profiles as predicted by CFD, the parameterization introduced in the present report, and the parameterization of Ainslie, as given by the legend in the top-left graph. The streamwise location at which these profiles are predicted is given by the title at the top of each column of axes, while the blockage ratio of the simulation is given to the right of . . .*

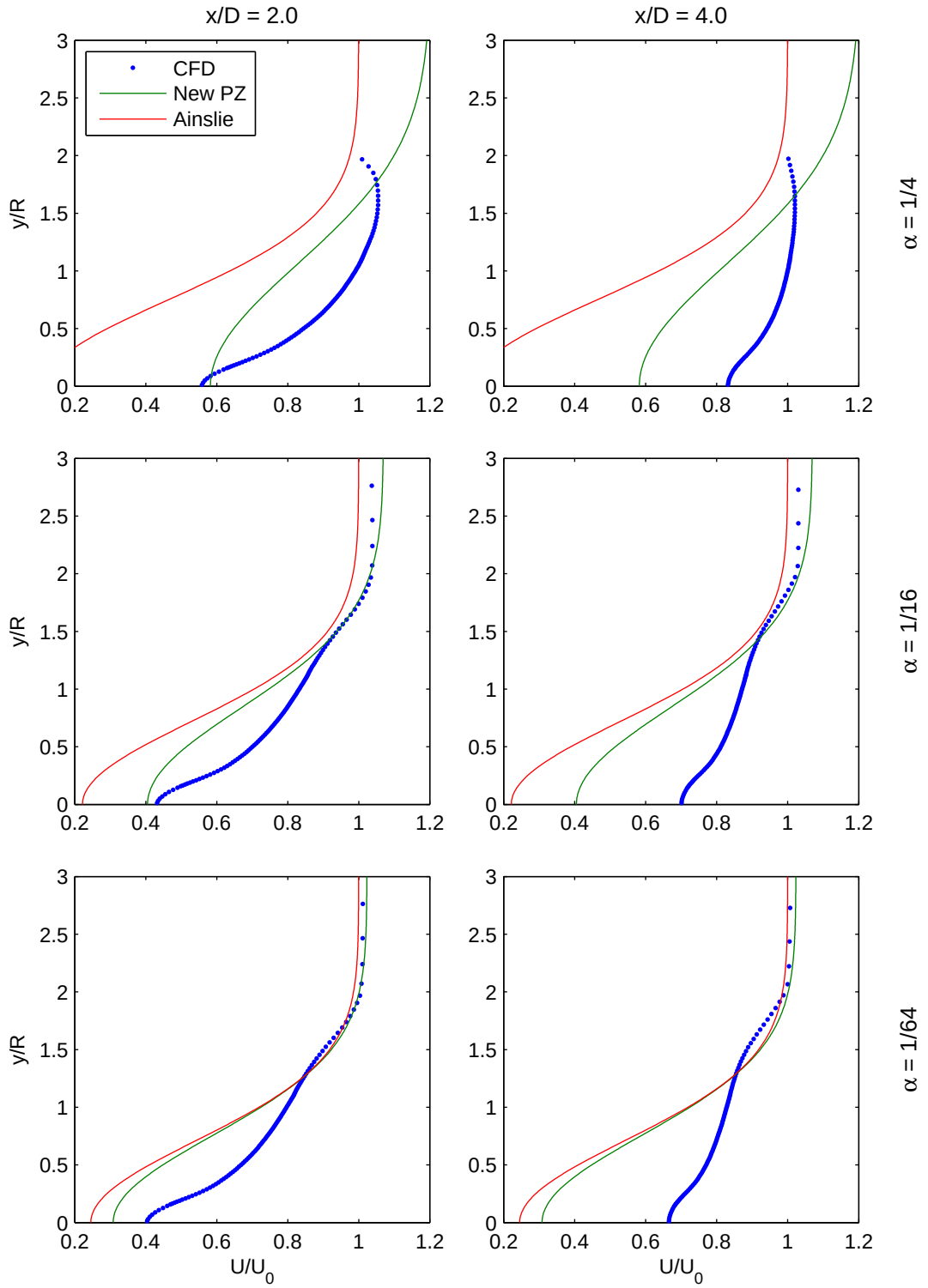


**Figure 8 (ctd.):** *. . . each row of axes. Each graph therefore represents the predictions for a specific location in a specific simulation. The tip speed ratio in all simulations is 5.0, with the thrust coefficients being 1.11, 0.98 and 0.95 for blockage ratios of 1/4, 1/16 and 1/64 respectively.*

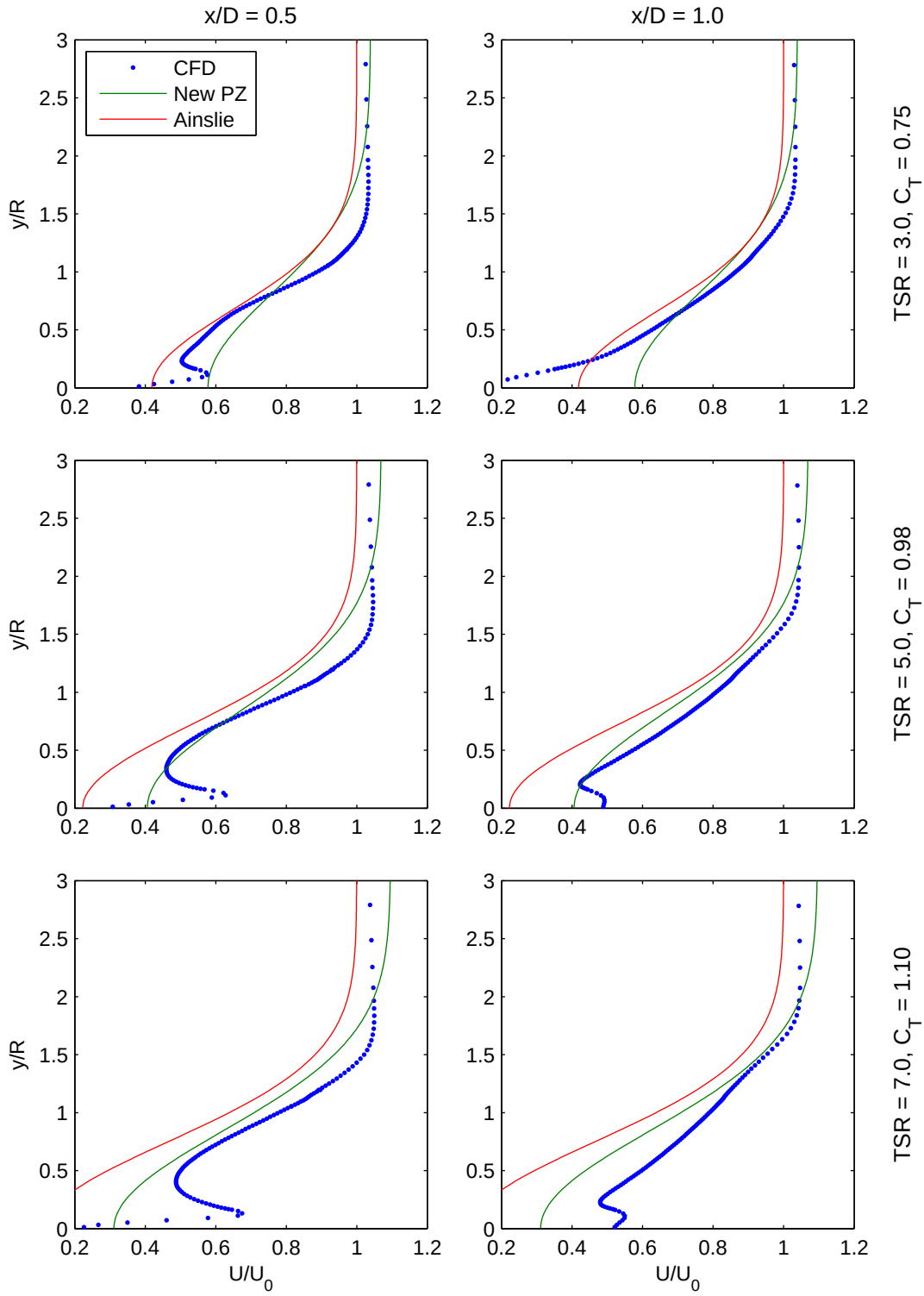


**Figure 9:** *Lateral wake profiles as predicted by CFD, the parameterization introduced in the present report, and the parameterization of Ainslie, as given by the legend in the top-left . . .*

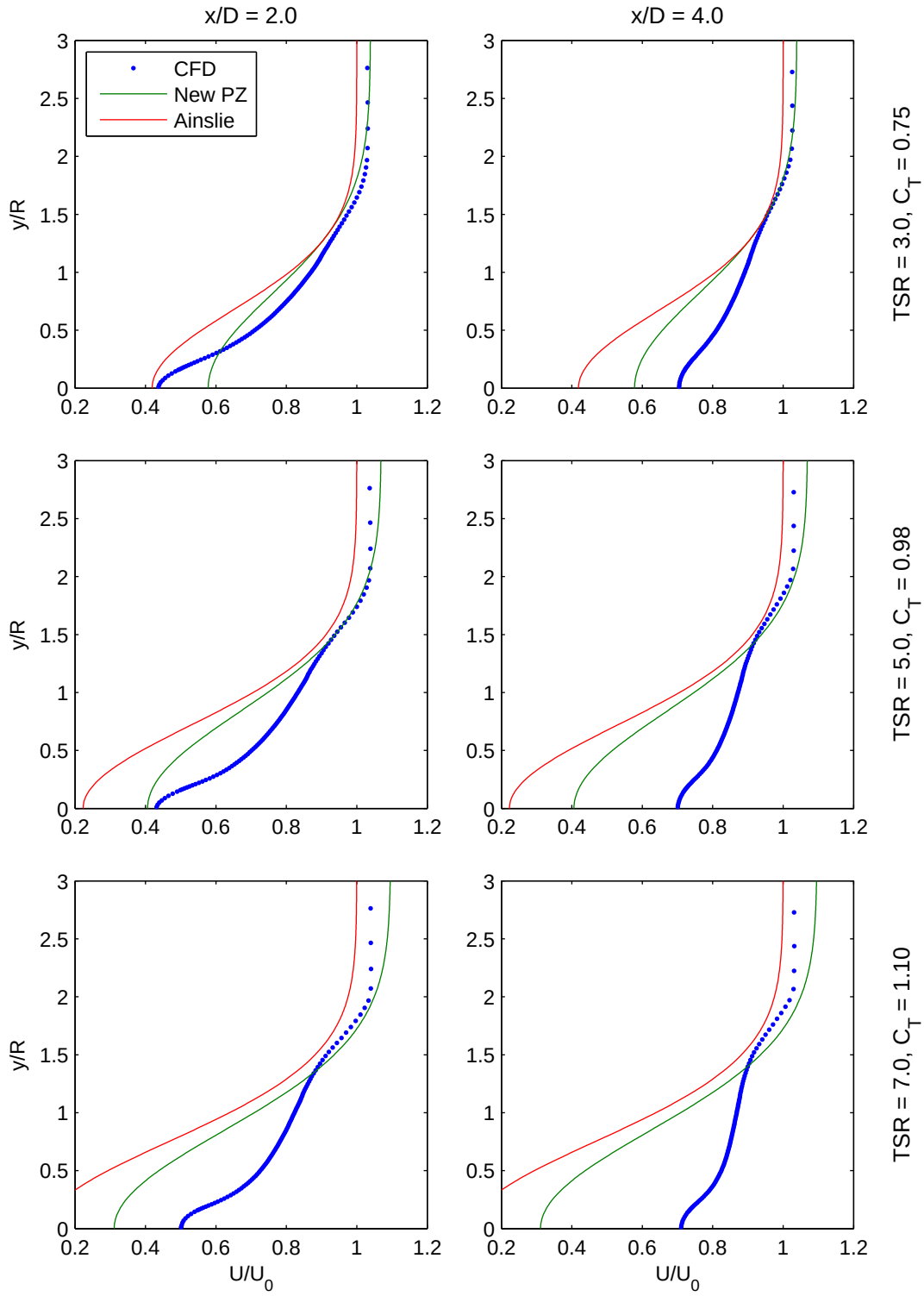


**Figure 9 (ctd.):** *. . . graph. The arrangement is as per Figure 8, except that the simulations now differ by tip speed ratio as opposed to blockage ratio, with the blockage ratio constant at 1/16.*

# 5 Parameterization of open-centre high-solidity turbine results from D2

The parameterization of the open-centre high-solidity turbine results from D2 is also based on the blockage model first introduced in D1. Whilst this turbine differs in three key aspects, namely, the open-centre, the high-solidity, and the addition of a duct, it is believed that, as a first approximation, the most important driving mechanics are still those included in the blockage model. The key difference in the wake which must be included is the presence of the relatively high speed centre flow, caused of course by the open centre of the turbine. As will be discussed below, this is included by treating this as part of the bypass flow.

Another consideration for the open-centre parameterization is the area reference used in the calculation of the thrust coefficient and blockage ratio, which are inputs to the blockage model. In the D2 report, the thrust and power coefficients were calculated based on the *throat* area of the duct, while the blockage ratio was not considered. For the present parameterization, it was felt appropriate that the area reference should be the frontal area of the turbine, as this is the equivalent area for the actuator disc. This means that the thrust and power coefficients given in the D2 report need to be divided by 0.75 i.e. multiplied by $1.\dot{3}$. The blockage ratio is 3.6% – somewhat lower than the 'medium' blockage for the low-solidity turbine.

## 5.1 Wake profile

The model profile adopted for the open-centre, high-solidity turbine parameterization is equivalent to that used for the conventional low-solidity turbine, but with the addition of an offset such that the peak is no-longer at $r = 0$, but instead at $r = \mu$:

$$\begin{aligned} \Delta\widetilde{U}_w &= (\Delta\widetilde{U}_{w\sqcap} - \Delta\widetilde{U}_{bp\sqcap}) \exp\left(-\frac{1}{2}\left(\frac{r-\mu}{\sigma R}\right)^2\right) + \widetilde{U}_{bp\sqcap} \\ &= A_1 \exp(-Bt^2) + A_2 \end{aligned} \tag{37}$$

where:

$$A_1 = \Delta\widetilde{U}_{w\sqcap} - \Delta\widetilde{U}_{bp\sqcap} \tag{38}$$

$$A_2 = \Delta\widetilde{U}_{bp\sqcap} \tag{39}$$

$$B = 1/(2\sigma^2 R^2) \tag{40}$$

as before, and $t = r - \mu$. The substitution variable $t$ is introduced in order to simplify the integration. Note that the value of $\mu$ must be specified as an input to the parameterization i.e. its value is not determined as part of the parameterization model.

The limits for the integral are found by equating Equation 37 to zero to give:

$$\begin{aligned} r^-/R &= \max(\mu/R - C_1\sigma, 0) \\ r^+/R &= \mu/R + C_1\sigma \end{aligned} \tag{41}$$

where:

$$C_1 = \sqrt{-2\ln\left(\frac{-A_2}{A_1}\right)} \tag{42}$$

Note also that the lower limit $r^-$ cannot be negative as this would not make physical sense.

As before, the momentum flux deficit given by this profile is found by integration. Starting with:

$$\Delta\dot{M} = \rho 2\pi U_\infty^2 \int_{r^-}^{r^+} r\Delta\widetilde{U}_w(1 - \Delta\widetilde{U}_w)\,\mathrm{d}r \tag{43}$$

we substitute Equation 37 and change the integration variable and limits from $r$ to $t$ to give:

$$\Delta\dot{M} = \rho 2\pi U_\infty^2 \int_{t^-}^{t^+} (t+\mu)(A_1\exp(-Bt^2) + A_2)(1 - A_1\exp(-Bt^2) - A_2)\,\mathrm{d}t \tag{44}$$

Making use of the result:

$$\int t\exp(-Bt^2)\,\mathrm{d}t = -\frac{\exp(-Bt^2)}{2B} \tag{45}$$

as before, and also the result:

$$\int_0^x \exp(-Bt^2)\,\mathrm{d}t = \frac{\sqrt{\pi}}{2\sqrt{B}}\,\mathrm{erf}(\sqrt{B}x) \tag{46}$$

where ‘erf’ is the error function, a non-elementary function which gives the definite integral of a Gaussian distribution, gives:

$$\begin{aligned}\Delta\dot{M} = \rho 2\pi U_\infty^2 \Bigg[ & \frac{1}{2B}(2A_1A_2 - A1)\exp(-Bt^2) \\ & + \frac{A_1^2}{4B}\exp(-2Bt^2) + \frac{1}{2}(A_2 - A_2^2)t^2 \\ & + \frac{\mu A_1\sqrt{\pi}}{2\sqrt{B}}(1 - 2A_2)\,\mathrm{erf}(\sqrt{B}\,t) \\ & - \frac{\mu A_1^2\sqrt{\pi}}{2\sqrt{2B}}\,\mathrm{erf}(\sqrt{2B}\,t) + \mu A_2 t(1 - A_2) \Bigg]_{t^-}^{t^+}\end{aligned} \tag{47}$$

Substituting $B = 1/(2\sigma^2R^2)$, $t = r - \mu$, and normalizing as before, gives:

$$\begin{aligned}\Delta\widetilde{\dot{M}} = \Bigg[ & 4\sigma^2(2A_1A_2 - A1)\exp\left(-\frac{1}{2}\left(\frac{r-\mu}{\sigma R}\right)^2\right) \\ & + 2A_1^2\sigma^2\exp\left(-\left(\frac{r-\mu}{\sigma R}\right)^2\right) + 2(A_2 - A_2^2)\left(\frac{r-\mu}{R}\right)^2 \\ & + 2\sqrt{2}\sqrt{\pi}A_1\sigma\frac{\mu}{R}(1 - 2A_2)\,\mathrm{erf}\left(\frac{1}{\sqrt{2}}\left(\frac{r-\mu}{\sigma R}\right)\right) \\ & - 2\sqrt{\pi}A_1^2\sigma\frac{\mu}{R}\,\mathrm{erf}\left(\frac{r-\mu}{\sigma R}\right) + 4A_2\frac{\mu}{R}\frac{r-\mu}{R}(1 - A_2) \Bigg]_{(r^- - \mu)/R}^{(r^+ - \mu)/R}\end{aligned} \tag{48}$$

As before, the width of the Gaussian, $\sigma$, is then given by equating this with the momentum flux deficit from the top-hat profile Equation 22. A direct solution to this is however only possible if $r^-/R = \mu/R - C_1\sigma$ (as opposed to $r^-/R = 0$). This is because, if $r^-/R = 0$, there will be $\sigma$ terms outside and inside of the exponential and error functions, meaning that the $\sigma$ terms cannot be collected.

In the absence of a direct solution, an iterative solution is readily achieved, whereby a value for $\sigma$ is guessed, the Gaussian profile momentum flux deficit calculated and compared with the top-hat value, and the value of $\sigma$ then updated as appropriate. This is how this parameterization has been implemented by the present author.

## 5.2 Comparison with D2 results

The D2 report includes a study of the effect of the tip speed ratio at a fixed blockage ratio of approximately 3.6%. The tip speed ratio was varied from 2.2 to 3.4 giving thrust coefficients between 0.55 and 0.25 (based on the throat area) or 0.73 and 0.33 (based on the turbine frontal area). A comparison between these CFD results and the present parameterization is given in Figure 10 for three different tip speed ratios/thurst coefficients. The offset factor $\mu/R$ is equal to 0.8 in all cases, this having been manually adjusted to give the best visual agreement.

As with the low solidity parameterization, the agreement is best for $x/D = 1.0$. At this location the agreement for the centreline velocity deficit is very good for all of the tip speed ratios/thrust coefficients, suggesting that the centreline velocity deficit in the low-solidity turbine case may indeed be complicated by the relatively large nacelle (as compared to nacelles on wind turbines). More generally, it might also be the case that results with lower thrust coefficients and lower blockage ratios are better represented by the parameterization. Less well represented by the parameterization is the width of the wake, with the parameterization consistently over-predicting this. Indeed, the wake at $x/D = 1.0$ is clearly skewed, and so an alternative model profile would be required to represent this. At the next location downstream, $x/D = 2.0$, the wake has though become more nearly Gaussian.

Overall it is felt that the parameterization adequately captures the trends, and that the width could be readily tuned by the addition of adjustment factors. As with the parameterization of the low-solidity turbine, this has not been included in the present work as it will form part of D4.

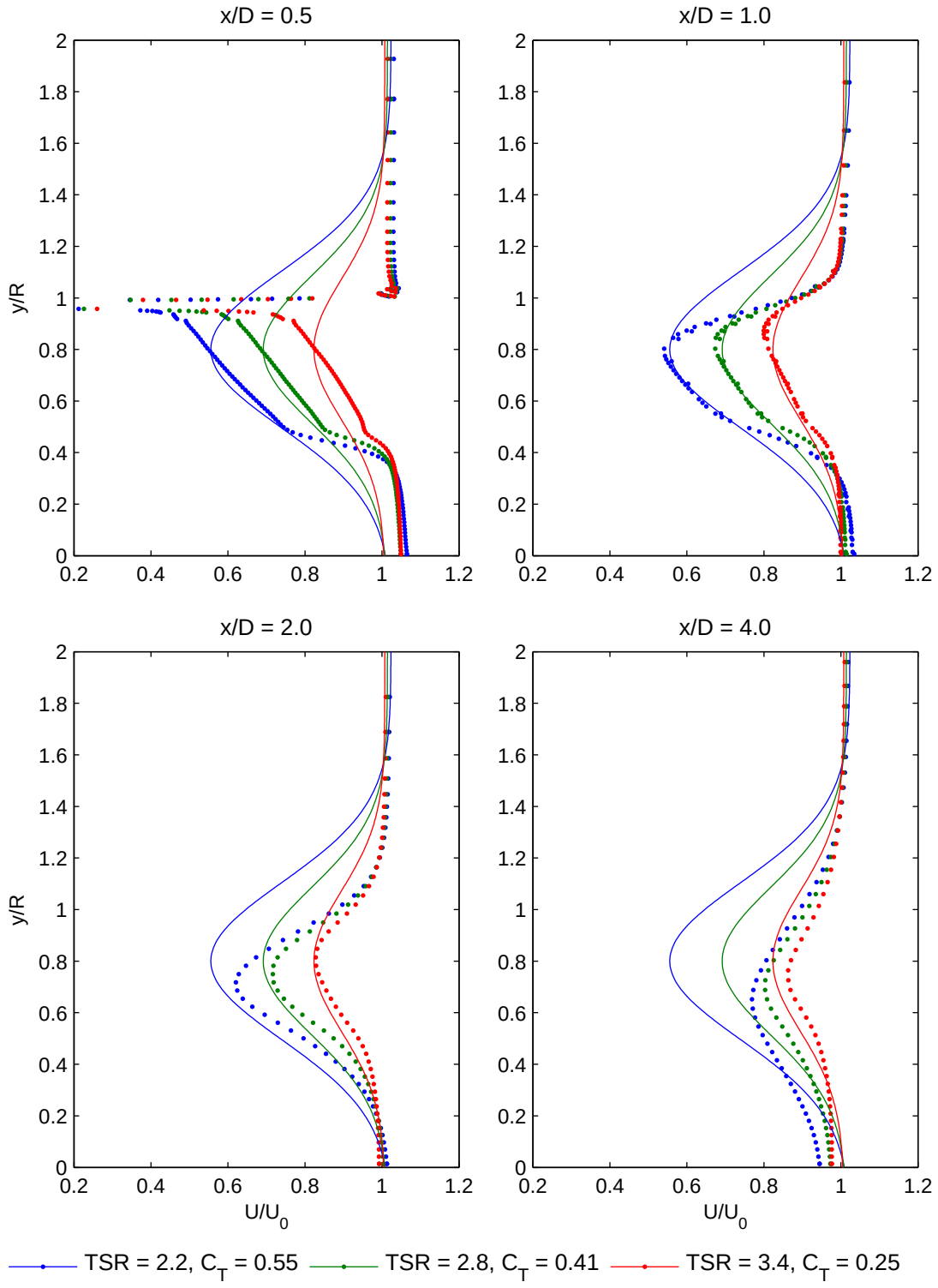


**Figure 10:** *Lateral wake profiles at four downstream locations, as indicated by the axes titles, and for* three different tip speed ratios/thrust coefficients*, as indicated by the legend. CFD data are give by dots while the parameterization is given by the continuous line. Thrust coefficients are based on the turbine area. The offset factor $\mu/R$ is equal to 0.8 in all cases.*

# 6 Conclusions

Presented above is a detailed literature review of the wake parameterizations in use in the field of wind energy, the development of new parameterizations applicable to the blocked flows in which tidal current turbines operate, and the comparison of these parameterizations with the CFD results for a low-solidity turbine from D1, and the results for an open-centre, high-solidity turbine from D2.

Three commonly used wake parameterizations were analysed in the literature review, and the key features of each identified. It was concluded that the most interesting features of the parameterizations considered were the use of an actuator disc model to inform the centreline velocity deficit (as per Schepers, 2003), and the principle of calculating the width of a Gaussian velocity deficit profile based on conservation of momentum principles (as per Ainslie, 1988). Further, and based on the conclusions of the D1 report, the requirement of incorporating a blockage model into the parameterization was identified.

The parameterizations developed for the two turbine geometries being studied in this work package, both of which are based around the blockage model documented in the D1 report, have been compared to the CFD results from D1 and D2. Overall, it is found that the agreement between the parameterizations and the CFD results is good, with the sensitivity of the wake deficit to the thrust coefficient and blockage ratio being correctly predicted. Broadly, the level of agreement between the parameterization introduced in this report and the CFD data to which it is compared is in line with the comparisons made between the wind turbine parameterizations in the literature and experimental data. It might also be reiterated that the present parameterization (for the low solidity turbine) is a better match to the CFD results that Ainslie's wind turbine parameterization.

Out of all of the comparisons made between the parameterizations and the CFD results, the most problematic is that for the low-solidity turbine, with the highest blockage ratio. This is shown in Figure 6. It seems likely that this is due to the combination of the high blockage ratio and relatively high thrust coefficient which both stretch the applicability of the blockage model. It may also be due to the specification of the velocity on the circumferential boundary in the CFD model. To an extent, this artificially increases the effective blockage by constraining the velocity, and causing the profile to curve back towards $U/U_o = 1$ on the circumferential boundary. Whilst these boundary conditions were used throughout the CFD work, it is only in

this highest blockage ratio case that it causes a problem. Notwithstanding this, the centreline velocity deficit is well predicted.

The possibility of using tuning factors in the parameterization to improve the agreement with the CFD results has been mentioned. Such an approach was used by Schepers, and, as has been pointed out, this leads to a situation where the normalized momentum flux deficit is no longer equal to the thrust coefficient on the turbine. This suggests that there are other processes at play, presumably the shear layer with the ground boundary. Ideally these processes would be incorporated into the parameterization. Looking forwards to D4, such tuning factors may be used to address the sensitivity of the wake to the ambient turbulence levels, as there is no sensitivity to this in the inviscid blockage model.

Again looking forwards to D4, it is expected that varying the turbulence intensity will lead to the location at which the parameterization best compares with the CFD results varying somewhat. The end-of-near-wake region is normally thought to lie closer to $x/D \approx 2$ whereas for the present results this is $x/D \approx 1$.

Finally, it is concluded that the present parameterization, developed in consultation with GL Garrad Hassan, is appropriate for WG3 WP4, as required by the acceptance criteria. Specifically, the parameterization describes all of the parameters which are required by GL Garrad Hassan's parabolized wake model.

# References

Ainslie, J. F. (1984), A wake interaction model for calculating cluster efficiencies, in *Proceedings of the 6th BWEA Wind Energy Conference*, CUP, Reading, UK.

Ainslie, J. F. (1985), Development of an eddy viscosity model for wind turbine wakes, in *Proceedings of the 7th BWEA Wind Energy Conference*, MEP, Oxford.

Ainslie, J. F. (1986), Wake modelling and the prediction of turbulence properties, in *Proceedings of the 8th BWEA Wind Energy Conference*, MEP, Cambridge.

Ainslie, J. F. (1988), Calculating the flowfield in the wake of wind turbines, *Journal of Wind Engineering and Industrial Aerodynamics*, 27, pp. 213–224.

Barthelmie, R. J., Folkerts, L., Larsen, G. C., Rados, K., Pryor, S. C., Frandsen, S. T., Lange, B., and Schepers, G. (2006), Comparison of wake model simulations with offshore wind turbine wake profiles measured by sodar, *Journal Of Atmospheric And Oceanic Technology*, 23, pp. 888–901.

Barthelmie, R. J., Hansen, K., Frandsen, S. T., Rathmann, O., Schepers, J. G., Schlez, W., Phillips, J., Rados, K., Zervos, A., Politis, E. S., and Chaviaropoulos, P. K. (2009), Modelling and measuring flow and wind turbine wakes in large wind farms offshore, *Wind Energy*, 12, pp. 431–444, DOI: 10.1002/we.348.

Burton, T., Sharpe, D., Jenkins, N., and Bossanyi, E. (2001), *Wind Energy Handbook*, Wiley.

Glauert, H. (1926), The analysis of experimental results in the windmill brake and vortex ring states of an airscrew, Reports & Memoranda No. 1026, Aeronautical Research Committee.

Gretton, G. I. (2011a), Development of a computational fluid dynamics model for a horizontal axis tidal current turbine – PerAWaT WG3 WP5 D1, Version 3.0, 12$^{th}$ December.

Gretton, G. I. (2011b), Development of a computational fluid dynamics model for an open-centre tidal current turbine – PerAWaT WG3 WP5 D2, Version 2.0, 9$^{th}$ December.

Jensen, N. O. (1983), A note on wind generator interaction, Report Risø-M-2411, Risø National Laboratory, Roskilde, Denmark.

Katić, I., Højstrup, J., and Jensen, N. O. (1986), A simple model for cluster efficiency, in *Proceedings of the 7th European Wind Energy Association Conference*, Rome, Italy.

Lange, B., Waldl, H.-P., Guerrero, A. G., Heinemann, D., and Barthelmie, R. J. (2003), Modelling of offshore wind turbine wakes with the wind farm program FLaP, *Wind Energy*, 6, pp. 87–104, DOI: 10.1002/we.84.

Mikkelsen, R. (2003), *Actuator disc methods applied to wind turbines*, Ph.D. thesis, Department of Mechanical Engineering, Technical University of Denmark.

Schepers, J. G. (2003), ENDOW: Validation and improvement of ECN's wake model, Technical Report ECN-C-03-034, Energy Research Centre of the Netherlands.

Thomson, M. D. (2010), GH near wake modelling report – PerAWaT WG3 WP4 D2, Document number 104329/BR/02, 15th June.